Journal of Biomechanics 82 (2019) 346–356

Contents lists available at ScienceDirect

Journal of Biomechanics

journal homepage: www.elsevier.com/locate/jbiomech
www.JBiomech.com

Virtual trial to evaluate the robustness of cementless femoral stems to patient and surgical variation ☆

Rami M.A. Al-Dirini [a,*], Saulo Martelli [a], Dermot O'Rourke [a], Daniel Huff [b], Ju Zhang [c], John G. Clement [d], Thor Besier [c], Mark Taylor [a]

[a] Medical Device Research Institute, College of Science and Engineering, Flinders University, Adelaide 5043, Australia
[b] DePuy Synthes, Johnson and Johnson, Warsaw, USA
[c] Auckland Bioengineering Institute, Auckland University, Auckland, New Zealand
[d] Melbourne Dental School, University of Melbourne, Melbourne, Australia

ARTICLE INFO

Article history:
Accepted 7 November 2018

Keywords:
Hip replacement
Implant design
Surgical planning
Finite element modelling
Primary stability
Patient factors
Implant robustness

ABSTRACT

Primary stability is essential for the success of cementless femoral stems. In this study, patient specific finite element (FE) models were used to assess changes in primary stability due to variability in patient anatomy, bone properties and stem alignment for two commonly used cementless femoral stems, Corail® and Summit® (DePuy Synthes, Warsaw, USA). Computed-tomography images of the femur were obtained for 8 males and 8 females. An automated algorithm was used to determine the stem position and size which minimized the *endo*-cortical space, and then span the plausible surgical envelope of implant positions constrained by the *endo*-cortical boundary. A total of 1952 models were generated and ran, each with a unique alignment scenario. Peak hip contact and muscle forces for stair climbing were scaled to the donor's body weight and applied to the model. The primary stability was assessed by comparing the implant micromotion and *peri*-prosthetic strains to thresholds (150 μm and 7000 με, respectively) above which fibrous tissue differentiation and bone damage are expected to prevail. Despite the wide range of implant positions included, FE prediction were mostly below the thresholds (medians: Corail®: 20–74 μm and 1150–2884 με, Summit®: 25–111 μm and 860–3010 με), but sensitivity of micromotion and interfacial strains varied across femora, with the majority being sensitive ($p < 0.0029$) to average bone mineral density, cranio-caudal angle, post-implantation anteversion angle and lateral offset of the femur. The results confirm the relationship between implant position and primary stability was highly dependent on the patient and the stem design used.

1. Introduction

Total hip replacement (THR) is a successful operation that restores mobility and alleviates pain for patients with symptomatic end-stage hip disease (Learmonth et al., 2007). The number of THRs performed each year has reached approximately 1 million (Troelsen et al., 2013) and is predicted to almost double by 2030 (Kurtz et al., 2007). Cementless femoral stems are used in the vast majority of THRs performed on patients younger than 70 years (Wechter et al., 2013). The short- and long-term success for cementless stems have been associated with achieving primary stability (Maloney et al., 1989; Martelli et al., 2012; Pilliar et al., 1986b; Soballe et al., 1993), which requires good osseointegration between the bone and the stem. Aseptic loosening is the main reason for early revision of cementless femoral stems (Eskelinen et al., 2005) and can arise from adverse fibrotic tissue formation or *peri*-prosthetic bone damage. Fibrotic tissue formation is likely due to large micromotion between the stem and the hosting bone (Pilliar et al., 1986b), while *peri*-prosthetic bone damage is likely due to excessive strains on the host bone (Morgan and Keaveny, 2001). There is evidence that patient and surgical factors, including anatomy (Heller et al., 2001; Renner et al., 2016; Umeda et al., 2003), bone material properties (Wong et al., 2005), stem position (Bah et al., 2009; Bah et al., 2011; Dopico-Gonzalez et al., 2009), size (Al-Dirini et al., 2018) and the extent of the cortical contact (Viceconti et al., 2001b) influence micromotion, *peri*-prosthetic bone strains and hence, the primary stability of femoral stems.

☆ We certify that this article is original, that it is not under consideration by another journal or been previously published. All named authors were involved in the conception of the idea, data collection, data analysis and drafting of the final manuscript.

* Corresponding author.
E-mail addresses: rami.aldirini@flinders.edu.au (R.M.A. Al-Dirini), mark.taylor@flinders.edu.au (M. Taylor).

https://doi.org/10.1016/j.jbiomech.2018.11.013
0021-9290/

Studying the influence of patient and surgical factors on the primary stability requires the exploration of a wide range of possible scenarios in implant position, host bone morphology and material properties (Taylor et al., 2013). While clinical trials on large patient cohorts allow for studying the combined influence of variation in patient and surgical factors as they inherently capture a wide range of possible scenarios (Mahmood et al., 2016; Pagnano et al., 1996; Russotti and Harris, 1991; Vicenti et al., 2016), it is difficult to separate the influence of surgical factors from that of patient factors. Generating patient-specific finite element (FE) modelling from Computer Tomography (CT) images is an established and validated procedure for evaluating cortical strains (RSME = 180 με; (Taddei et al., 2010; Viceconti et al., 2000), micromovements (RSME = 10–20 μm; (Taddei et al., 2010; Viceconti et al., 2000) and *peri*-prosthetic bone strains (RSME = 400 με; (Viceconti et al., 2001a). Patient-specific FE modelling also has the potential to examine various surgical scenarios for each patient, as it allows for repeated use of the same specimen (Laz and Browne, 2010; Taylor et al., 2013). In addition, probabilistic analysis can be combined with patient-specific FE modelling to explore the effect of variability in patient and surgical factors on implant mechanics (Laz and Browne, 2010; Taylor et al., 2013). Such evaluation on implant stability is desirable early in the preclinical phases as it can potentially improve implant robustness to patient and surgical factors, and hence, reduce the risk of early failure in THRs. However, the majority of existing FE studies considered the influence of patient or surgical factors separately (Taylor and Prendergast, 2015), which does not allow the study of adverse interactions between patient and surgery related factors.

Computational FE studies focusing on patient factors have been performed on patient cohorts (Al-Dirini et al., 2017; Bah et al., 2015; Bryan et al., 2012; Lengsfeld et al., 2005; Pacanti et al., 2003; Wong et al., 2005), but often assume an ideal implant position (Taylor et al., 2013). Other studies have considered various surgical scenarios by changing the stem position and orientation, but have used simplistic methods for varying implant position, which do not account for individual *endo*-cortical boundaries that govern ranges of possible variation within the hosting bone (Bah et al., 2009; Bah et al., 2010; Bah et al., 2011; Dopico-Gonzalez et al., 2009, 2010a). In addition, these studies have been performed on a maximum of three patients, yet great variability in the sensitivity of the primary stability to implant position and orientation was observed across patients and implant designs. It remains unclear if the reported variability was due to differences in patient factors, implant designs used or in the methods applied. The reported variability also raises the question as to whether there is a consistent set of alignment factors that dominate the variability between stem designs, and across patients. Hence, the aim of this study was to investigate the influence of surgical variation on the primary stability of femoral stems across a diverse patient cohort that is representative of the range of variability in the general THR population. We hypothesize that there is a consistent set of implant alignment parameters that influence the micromotion and interfacial strains across patients. Therefore, FE analysis was performed on a representative cohort of femora, using two successful, contemporary femoral stems that are commonly used in cementless THR: Corail® and Summit® (DePuy Synthes, Warsaw, USA).

2. Methods

2.1. CT scans and loading

This study was approved by the Southern Adelaide Clinical Human Research Ethics Committee. CT scans for sixteen femora (8 male and 8 female femora) were selected from the Melbourne Femur Collection (MFC) (Clement, 2005). The selected femora were from individuals with age (51–71 years) and body mass index (19.3–36.8 kg m^{-2}) that are representative of the THR population (Clement, 2005). See Appendix A for details. All scans had a phantom (Mindways Software, Inc, Austin, USA), which consisted of five solid monomer rods, each with a known density and a different attenuation coefficient equivalent to a mixture of water and dipotassium phosphate (K_2HPO_4).

2.2. Finite-element modelling

Surfaces for the external and the inner bone cortex for each femur were generated based on manual segmentation of calibrated CT scans, using ScanIP (Simpleware, Exeter). The CT scans were calibrated as per the recommendation of the manufacturer (Mindways Software, Inc, Austin, USA) with cortical bone, water and air identified at 1650 HU, 0 HU and −1000 HU, respectively. Hounsfield values (HU) were sampled from the calibrated CT scans then converted to Young's moduli (E) using established HU-to-density and density-to-Young's modulus relations for the femoral neck developed by Morgan et al. (2003). Patient-specific FE models of intact femora were generated by mapping (ScanIP, Simpleware, Exeter) the Young's moduli onto first order tetrahedral meshes whose element size was equal to, or smaller than the voxel size of the CT scans (∼1 mm).

2.3. Analysis using reference implant position

Two sets of FE models for the implanted bone were generated; one with the standard offset collared Corail® stem and the other with the standard offset Summit® stem (Fig. 1). The geometry of the implanted femur was obtained via Boolean operations between the intact femur and the implant geometry in the reference position. The reference position was defined for each femur by the implant size and position which achieved maximum medullary canal fill, without breaching the cortical bone boundaries. Based on a previous mesh convergence study (Al-Dirini et al., 2017), linear tetrahedral meshing with edge lengths between 0.5 and 0.8 mm was performed on the implanted models using Hypermesh (Altair Engineering, Troy, MI). Linear elastic, heterogeneous material properties were interpolated from the intact femur models. Surface-to-surface contact that allowed large sliding (Viceconti et al., 2000) was implemented over the entire length of the stem, with a coefficient of friction of 0.6 (Dammak et al., 1997; Hashemi et al., 1996). Peak joint contact and muscle forces associated with stair ascent were taken from the work of Heller et al. (Heller et al., 2005), scaled to the body mass of the individual and applied to the models. The forces applied included the hip reaction force, the resultant of the abductors (i.e., the gluteus maximus, medius, minimus and tensor fascia latae), the resultant of the vastus lateralis muscle and the resultant of the ilio-tibial tract and the vastus medialis muscles. All models were rigidly constrained at the condyles (Heller et al., 2005).

2.4. Variation in implant position

For each model, the space between the stem and the *endo*-cortical bone surface was used to define the admissible ranges for surgical variation (Al-Dirini et al., 2018). Changes in stem position, relative to the reference model, were defined as changes of stem anteversion ($Antv_{angle}$: rotation about the y-axis), varus/valgus ($V\text{-}V_{angle}$: rotation about the x-axis), anterior/posterior rotations ($A\text{-}P_{angle}$: rotation about the z-axis), medial/lateral offset ($ML\ Offset_{IMP}$: translation in the z direction) and vertical offset ($SI\ Offset_{IMP}$: translation in the y direction). Changes to the V-

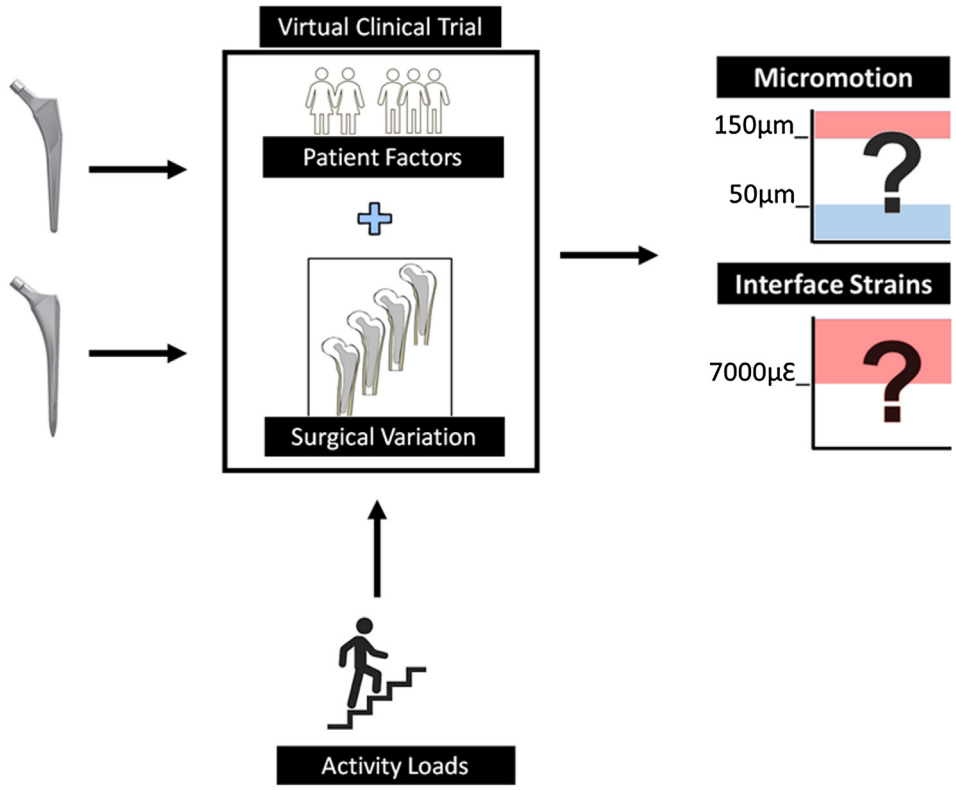

Fig. 1. Overview of the study design. Primary stability was assessed by comparing the FE predicted micromotion and interfacial strains to thresholds (red regions in plots on the right side of the figure) at which fibrous tissue differentiation and bone damage is expected to prevail. (For interpretation of the references to colour in this figure legend, the reader is referred to the web version of this article.)

V_{angle} and the A-P_{angle} were introduced by moving the location of the points defining the stem axis within the range for surgical variation (Fig. 2), whereas changes to the $Antv_{angle}$, the SI $Offset_{IMP}$ and the ML $Offset_{IMP}$ were introduced by moving the trunnion point within a spherical space of 20 mm diameter. An initial sample of 60 normally distributed surgical scenarios were generated for each femur-stem combination using Latin Hypercube sampling, resulting in a total of 1952 simulations (32 models with reference implant positions and 1920 models with surgical variations of the reference position).

2.5. Assessment of implant stability

Micromotion less than 50 μm promote osseointegration, whereas micromotion greater than 150 μm lead to the formation of soft fibrotic tissue (Pilliar et al., 1986a). These thresholds were

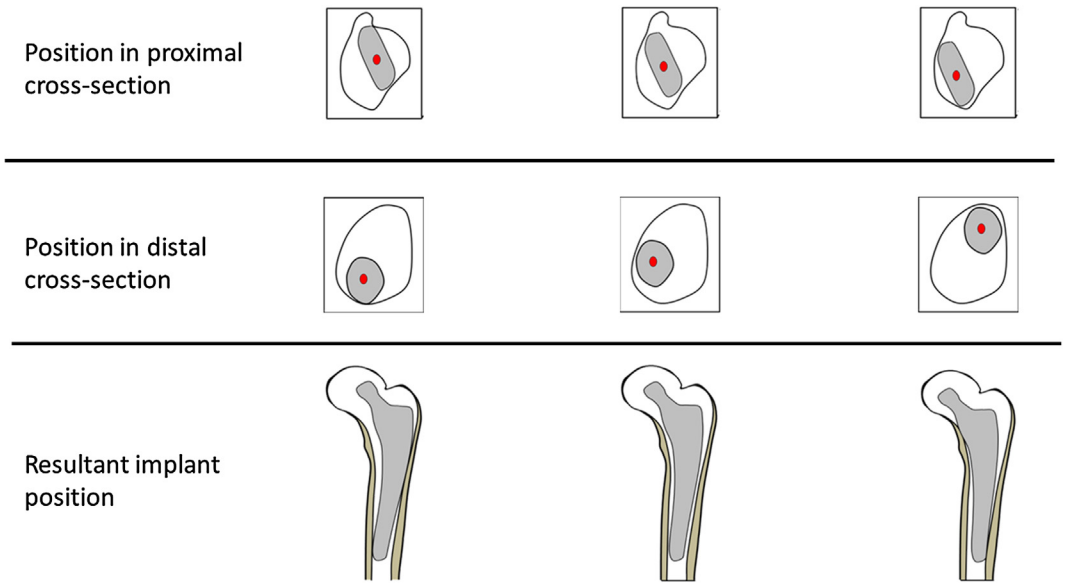

Fig. 2. Illustration of how stem position was varied in this study. In summary, proximal and distal cross-sections were taken of the implanted bone. Centroids for the 2D cross-sections of the stem were calculated, and were used to vary the stem position within the host bone. In addition, the head centre location was also varied to control the stem anteversion and offsets in the vertical and medial directions.

used to identifying regions of osseointegration and fibrous tissue formation, respectively. Also, the yield strain for bone, 7000 με (Bayraktar et al., 2004), was used as a threshold for identifying areas of potential bone damage. The median micromotion and strain over the bone-implant interface area were used as global indicators of stability, whereas the 90th percentiles of the distributions were used as local indicator of stability.

2.6. Assessment of the sensitivity of implant stability to surgical scenarios

For each patient, the influence of stem position on micromotion was evaluated by stratifying models into two groups with micromotion lower (MG1) and greater (MG2) than that of the reference model. Similarly, for each patient, the influence of stem position on the interfacial strains was evaluated by stratifying models into two groups with interfacial strains lower (SG1) and greater (SG2) than that of the reference model. Positioning parameters (V-V_{angle}, $Antv_{angle}$, A-P_{angle}, ML $Offset_{IMP}$ and SI $Offset_{IMP}$) in MG1/SG1 were compared with those in MG2/SG2 using Wilcoxon tests. Bonferroni correction was used to account for the multiple comparisons performed, with significance set at $p < 0.0029$. The analysis was repeated for Corail® and Summit®. The study hypothesis was tested by comparing the sensitivity of implant stability to positioning parameters, across the study cohort.

2.7. Assessment of the sensitivity of implant stability to patient factors

Results from the analysis combining patient and surgical variability were used to assess the sensitivity of implant stability to patient factors. Patient factors considered in this analysis were: body mass, stature, body mass index, average bone mineral density (BMD), native femur length, neck length, cranio-caudal angle (CCD), femoral anteversion, and femoral offset in the vertical and the medial directions. Initially, models were stratified into two groups with 90th percentile micromotion less than (safe group) and greater than 150 μm (at-risk group). 150 μm was taken as a threshold above which fibrous tissue is likely to form. However, performing the analysis using this stratification did not identify any patient factors contributing to the implant micromotion. Therefore, models were re-stratified into two groups as follows: (i) models with 90th percentile micromotion greater than 150 μm (at-risk group), and (ii) models with 90th percentile micromotion less than 50 μm (safe group), a threshold below which osseointegration is likely to occur. Micromotion between 50 μm and 150 μm remains a region of uncertainty, and hence, models with 90th percentile micromotion within this region were not included in this analysis. In light of this, the safe group refers to models that are likely to have bone osseointgration over the entire implant surface, and hence, are likely to achieve primary stability, whereas the at-risk group is likely to have fibrous tissue differentiation at some region of the implant surface, which may not necessarily lead to implant loosening and revision, but is taken as an indicator of the risk of implant loosening due to fibrous tissue differentiation.

Similarly, models were also stratified into two groups based on interfacial strains: (i) models with 90th interfacial strain percentile greater than bone yield threshold (7000 με) (at-risk group) and (ii) models with 90th percentile interfacial strains less than bone yield threshold (7000 με) (safe group). Again, the safe group refers to cases that are unlikely to experience *peri*-prosthetic bone damage,

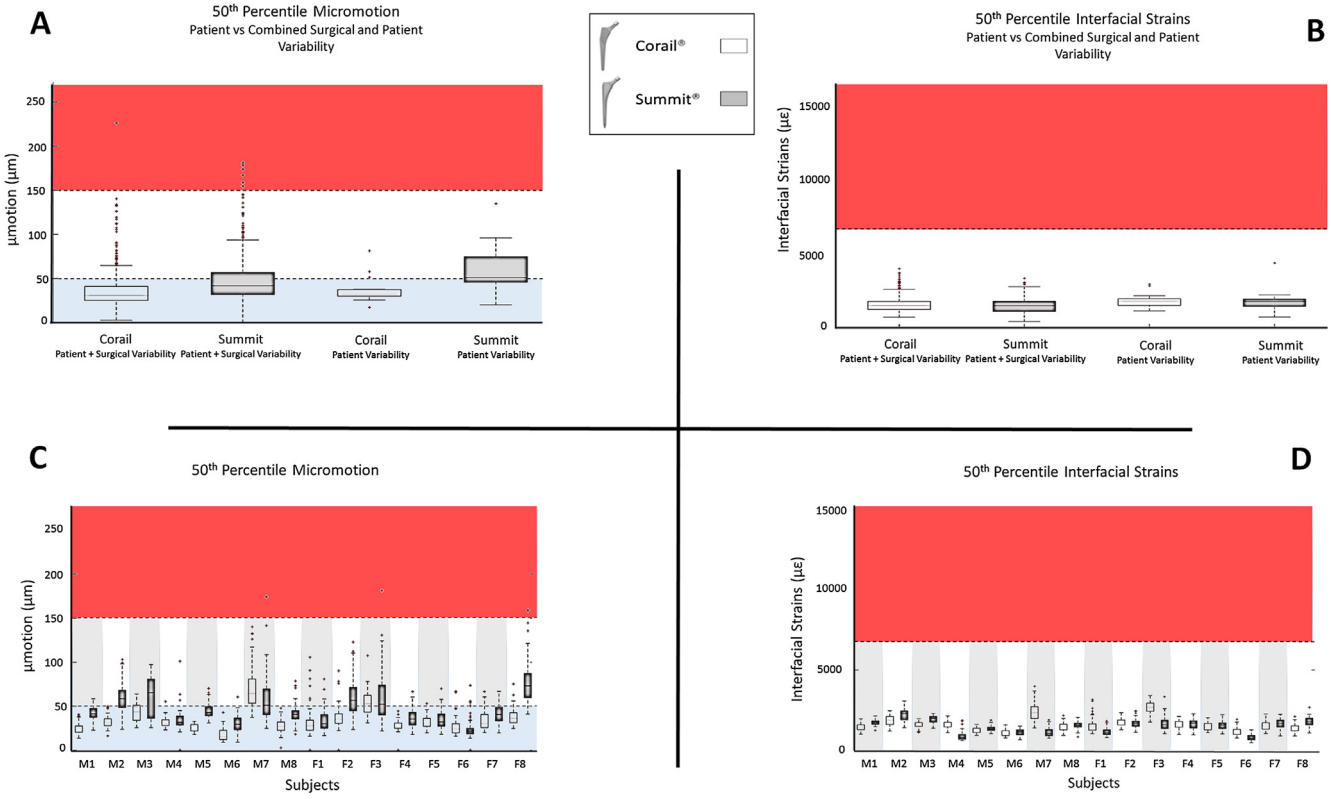

Fig. 3. Median micromotion (right) and interfacial strains (left) predicted for the entire study cohort (top) and for each subject in the study (bottom). The top plots show a comparison of variability in micromotion and interfacial strains, with and without surgical variability. For all plots, white/light boxes represent Corail® while grey/dark boxes represent Summit®. The red regions show thresholds for fibrous tissue differentiation and bone damage, while the light blue region shows micromotion threshold for good bone osseointegration with the stem surface. (For interpretation of the references to colour in this figure legend, the reader is referred to the web version of this article.)

whereas the at-risk group is likely to have some region at the contact interface with bone damage, which is taken as an indicator or the risk of implant loosening.

The at-risk group was compared to the safe group using Wilcoxon's tests for both micromotion and interfacial strains and both for Corail® and Summit® stems. Bonferroni correction was used to account for the multiple comparisons performed, with significance set at $p < 0.0029$. All analyses were run in Matlab (Mathworks, Nathick, USA).

3. Results

FE models of implanted femora were successfully generated and run for all 16 patients with implants in the ideal position. The analysis took approximately 65 CPU hours in total. The automated algorithm generated FE models for 60 different implant positions for each implant design, and for each femur in the cohort. The total CPU time required for the analysis was approximately 4000 h.

Differences were found between FE predictions using the reference implant position (only considering patient factors) and those predicted when considering the combined patient and surgical variability ($p < 0.001$). For the femora implanted in the reference position, the median micromotion and interfacial strains were below the thresholds of 150 μm and 7000 με, respectively (5th–95th percentiles of the distributions: Corail®: 17–61 μm and 910–2550 με, Summit®: 19–73 μm and 630–2110 με) (Fig. 3, A and B). For the analysis combining patient and surgical variability, the median micromotion and interfacial strains for the vast majority of the cases simulated were also less than 150 μm and 7000 με, respectively, for both stem designs, but with a greater variability in the ranges predicted (5th–95th percentiles of the distributions: Corail®: 20–74 μm and 1150–2884 με, Summit®: 25–111 μm and 860–3010 με) (Fig. 3A, 3B). Similar differences were noted for the 90th percentiles, with greater variability in micromotion and strain predicted by the combined analysis (Fig. 4A and 4B).

The combined analysis predicted similar number of models (and ranges) with 90th percentile micromotion less than 150 μm for both designs, with Corail® at 90% of simulated models (5th–95th percentiles of the distributions: 53–193 μm) and Summit® at 94% of simulated models (5th–95th percentiles of the distributions: 50–238 μm), respectively. The 90th percentile micromotion were less similar for the two stem designs, particularly the ranges of variability, when the reference position was only considered, with Corail® at 14/16 patients (5th–95th percentiles of the distributions: 17–61 μm) and Summit® at 13/16 patients (5th–95th percentiles of the distributions: 19–73 μm) (Fig. 3C and 4C) with 90th percentile micromotion less than 150 μm. Similar observations were noted for the interfacial strains (Fig. 3D, and 4D).

The predicted micromotion for Corail® was generally less than, or equal to those for the Summit®, especially for the median micromotion. However, it was noted that the use of Summit® resulted in a large reduction in micromotion and interfacial strains for one male (M7) and one female patients (F3), from mostly above to mostly below thresholds (150 μm and 7000με), particularly when the 90th percentile values were considered (Fig. 4C, 4D and Fig. 5). The same patients had median micromotion/strain predic-

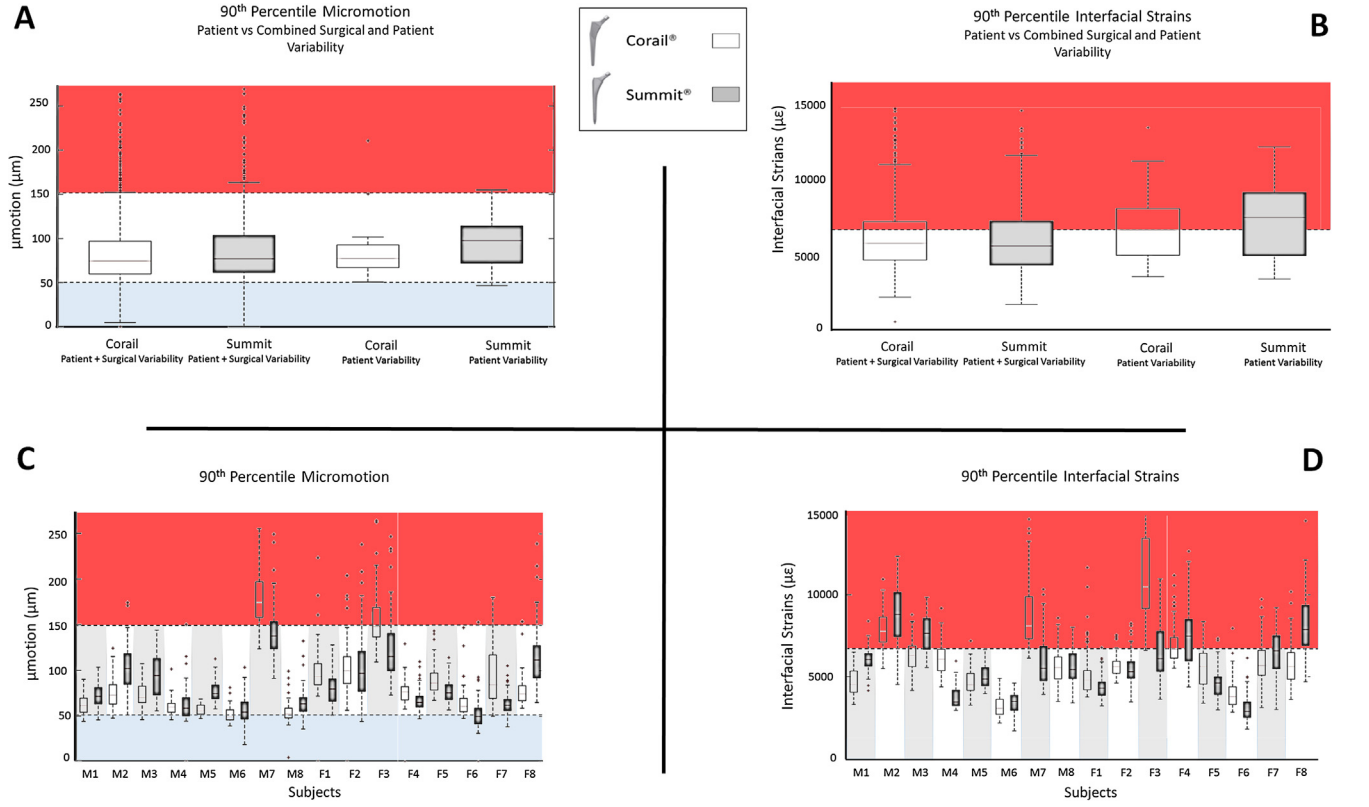

Fig. 4. 90th percentile distribution for micromotion (right) and interfacial strains (left) predicted for the entire study cohort (top) and for each subject in the study (bottom). The top plots show a comparison of variability in micromotion and interfacial strains, with and without surgical variability. For all plots, white/light boxes represent Corail® while grey/dark boxes represent Summit®. The red regions show thresholds for fibrous tissue differentiation and bone damage, while the light blue region shows micromotion threshold for good bone osseointegration with the stem surface. (For interpretation of the references to colour in this figure legend, the reader is referred to the web version of this article.)

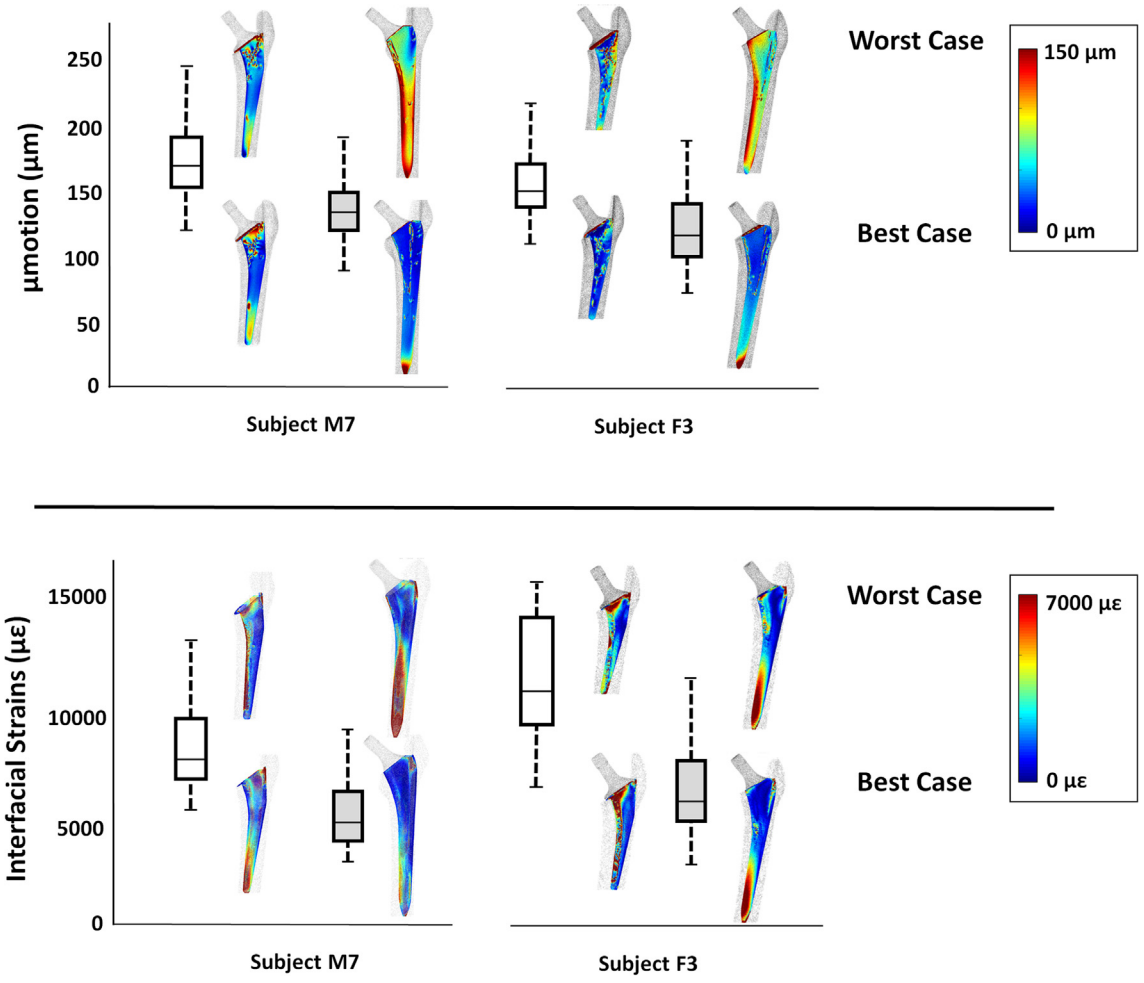

Fig. 5. Micromotion (top) and interfacial strain (bottom) distributions for the best- and worst-case scenarios for subjects with 90th micromotion/strain percentile profiles exceeding desired thresholds (subjects M7 and F3 from Fig. 4).

tions within acceptable ranges for both stem designs (Fig. 3A and 3B).

3.1. Sensitivity of micromotion and interfacial strains to surgical scenarios

The influence of implant position on the interfacial micromotion and strains was not uniform across the study cohort and implant designs. Nine patients (4 males and 5 females) were sensitive to changes in $Antv_{angle}$ ($p \ll 0.001$) and five male patients were sensitive to changes in ML $Offset_{IMP}$ ($p < 0.001$) with the Corail® stem (Fig. 6). Similarly, five patients (2 males and 3 females) were sensitive to changes in $Antv_{angle}$ ($p \ll 0.001$) and four male patients were sensitive to changes in ML $Offset_{IMP}$ ($p < 0.001$) with the Summit® stem (Fig. 6). Also, only one male patient was sensitive to changes in SI $Offset_{IMP}$ ($p = 0.0024$) and another male to changes in A-P_{angle} ($p = 0.0026$). None of the patients were found sensitive to changes in V-V_{angle} ($p > 0.02$). Similarly, six (2 males and 4 females) and five patients (2 males and 3 females) were sensitive to changes in ML $Offset_{IMP}$ ($p < 0.001$) when the Corail® and Summit® stems were used, respectively (Fig. 6). In contrast, only two patients (1 male and 1 female) using Corail® and two patients (1 male and 1 female) using Summit® were sensitive to changes in $Antv_{angle}$ ($p \ll 0.001$ - Fig. 7). Also, only one male patient was sensitive to changes in SI $Offset_{IMP}$ ($p = 0.0024$) and another to changes in A-P_{angle} ($p = 0.0026$). None of the patients were found sensitive to changes in V-V_{angle} ($p > 0.02$). Note that the aforementioned numbers of subjects showing sensitivity to each parameter were based on statistically significant differences.

3.2. Sensitivity of micromotion and interfacial strains to patient factors

Statistical analysis on patient factors found that micromotion and interfacial strains were sensitive to the average bone density and the native vertical femoral offset ($p < 0.001$- Fig. 8). The at-risk groups had a median average bone density of 0.52 g/cm^3 (Corial®) and 0.55 g/cm^3 (Summit®) and a median femoral offset of 55 mm (Corail® and Summit®), whereas the safe groups had a median average bone density of 0.6 g/cm^3 (Corail® and Summit®) and a median femoral offset of 62 mm (Corail®) and 58 mm (Summit®). The micromotion were also sensitive to cranio-caudal (or CCD) angle of the femur, with medians of 130 (Corail®) and 132 degrees (Summit®) for the at-risk groups, and 128 degrees (Corail® and Summit®) for the safe groups.

4. Discussion

The study identified several patient and surgical factors that influenced the interfacial micromotion and strain, and hence the primary stability of cementless femoral stems. Stem alignment influenced implant micromotion and interfacial strains leading to

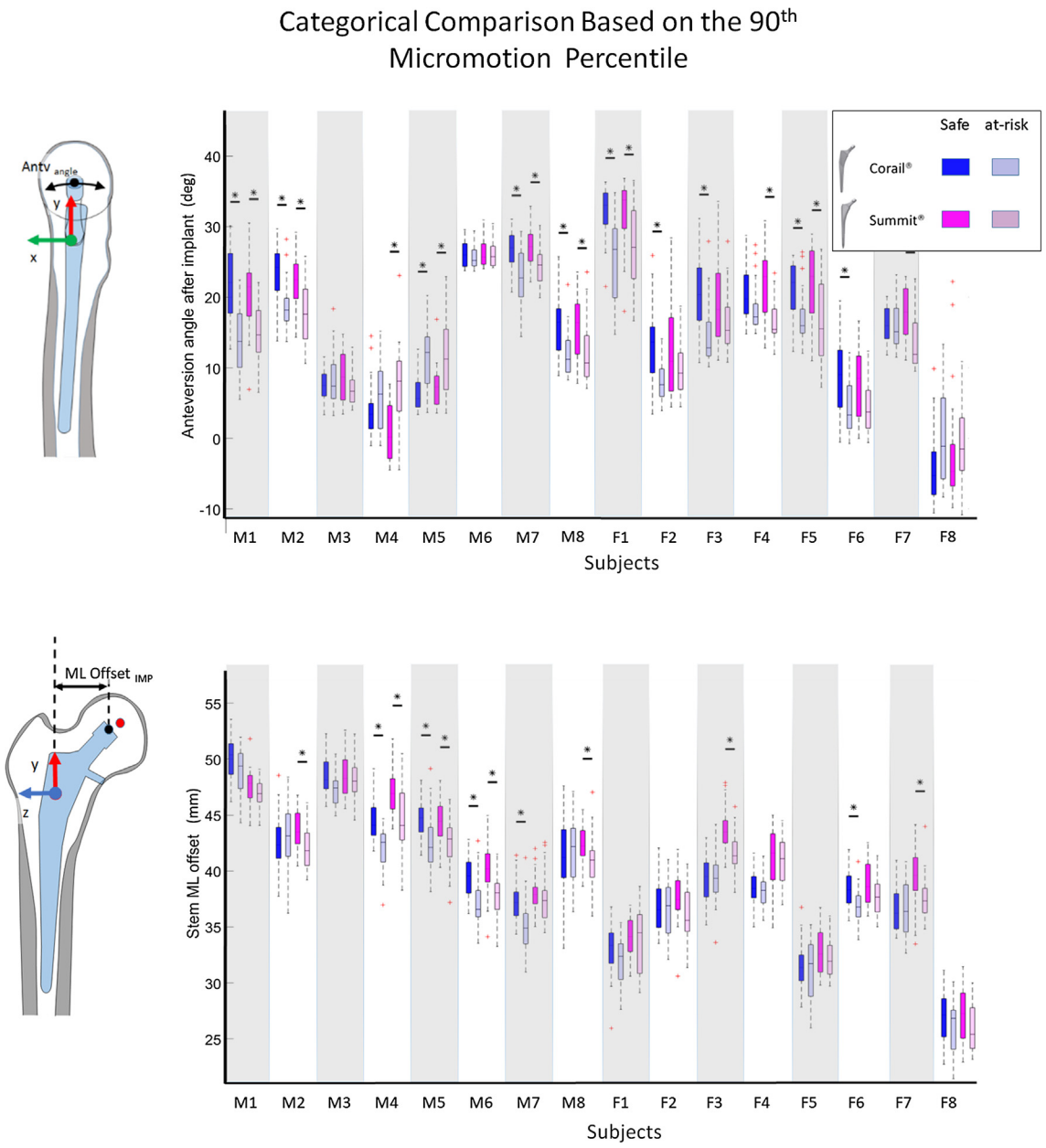

Fig. 6. 90th percentile micromotion profiles for Corail® and Summit®. M1–M8 are identifiers for males included in the study, while F1–F8 are identifiers for females in the study. Dark coloured (blue for Corail® and magenta for Summit®) boxes are used for the safe groups, while light coloured (blue for Corail® and magenta for Summit®) boxes show ranges for the at-risk groups. For each subject, the first two boxes (dark and light blue) are for Corail®, while the second (dark and light magenta) are for Summit®. This is for all subjects. ML $Offset_{IMP}$ refers to the implanted femoral offsets in the ML direction. The y-axis for both plots show the implanted Anteversion angles and ML $Offset_{IMP}$ of the implanted femora, measured relative to the native anatomy. A * indicates significant differences were found using Wilcoxon tests with Bonferroni correction. (For interpretation of the references to colour in this figure legend, the reader is referred to the web version of this article.)

changes in implant micromotion and bone strain up to 130 μm and 8000 με, for some patients. ML $Offset_{IMP}$ and $Antev_{angle}$ were the most common implant-alignment factors influencing the primary stability, with slightly retroverted and/or more medialised positions often leading to a reduction in micromotion, and sometimes, strains. This is consistent with previous findings on smaller cohorts (Al-Dirini et al., 2018; Dopico-Gonzalez et al., 2010b). Yet, this conclusion does not seem to be universal as reduction in micromotion/interfacial strains was noted for some patients when the stem was anteverted (M4, M5 and F8). Hence, the relationship between implant position and primary stability was highly dependent on the patient and the stem design used. The analysis performed also suggests that low BMD and/or CCD angles greater than 130 degrees as patient factors that may increase the risk of fibrous tissue differentiation and/or *peri*-prosthetic bone damage, due to excessive micromotion and strains.

The predicted median stem micromotion and *peri*-prosthetic bone strains were below thresholds for fibrous tissue differentiation and bone damage (Figs. 3 and 4), respectively, predicting good osseointegration between the stem and most of the *peri*-prosthetic bone surface. However, there were large differences in the predicted micromotion profiles between Corail® and Summit® (Fig. 3B and 4B), when only assessing the influence of patient variability. This seems to be inconsistent with the comparable clinical performance for Corail® and Summit® (Australian Orthopaedic Association National Joint Replacement Registry, 2015; Havelin

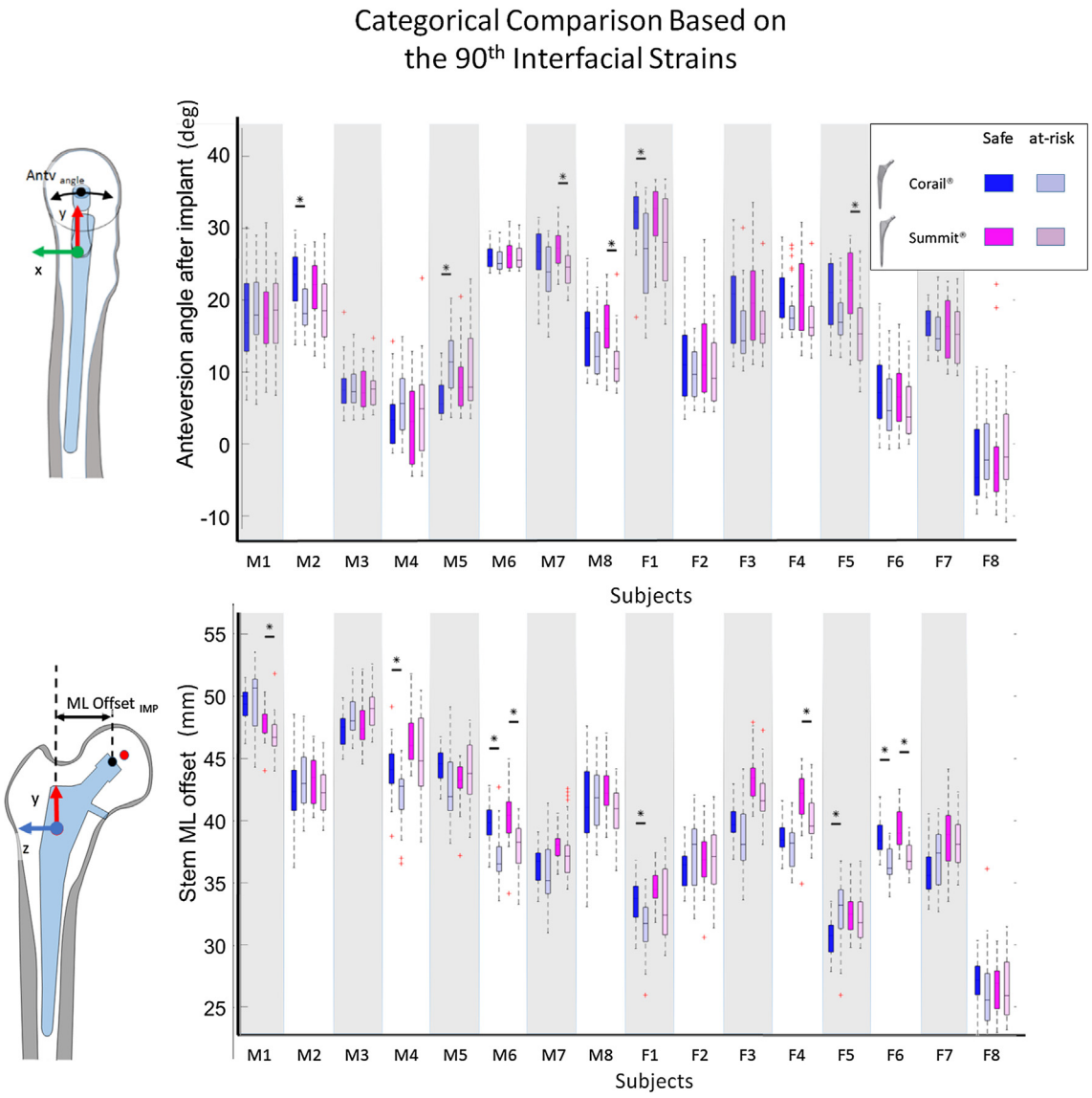

Fig. 7. Subject-specific 90th percentile interfacial strains for Corail® and Summit®. M1–M8 are identifiers for males included in the study, while F1–F8 are identifiers for females in the study. Dark coloured (blue for Corail® and magenta for Summit®) boxes are used for the safe groups, while light coloured (blue for Corail® and magenta for Summit®) boxes show ranges for the at-risk groups. For each subject, the first two boxes (dark and light blue) are for Corail®, while the second (dark and light magenta) are for Summit®. This is for all subjects. ML $Offset_{IMP}$ refers to the implanted femoral offsets in the ML direction. The y-axis for both plots show the implanted Anteversion angles and ML $Offset_{IMP}$ of the implanted femora, measured relative to the native anatomy. A^{*} indicates significant differences were found using Wilcoxon tests with Bonferroni correction. (For interpretation of the references to colour in this figure legend, the reader is referred to the web version of this article.)

et al., 1995), which have revision rates for aseptic loosening of 95.1% and 98.1% at 10 years, respectively. Inclusion of variability in stem position in addition to patient factors resulted in micromotion profiles that are similar for both stem designs, which better agrees with the known clinical history and National Joint Registries (NJR) records for the long-term survivorship for both stem designs (Australian Orthopaedic Association National Joint Replacement Registry, 2015; Havelin et al., 1995). This confirms the data generated in this study, particularly when surgical variation was included, can serve as a potential benchmark for future analyses on new stem designs.

Differences were observed between stem designs, particularly in the 90th percentile micromotion and strains, to the point that for some patients (M3, M7, F3, F7 and F8), the use of one design shifted the 90th percentile micromotion and strain profiles dramatically from mostly exceeding to mostly below thresholds for fibrous tissue differentiation and bone damage. Although these elevated values were affecting less than 10% of the implant contact surface, which is unlikely to introduce substantial changes to the primary stability, the large differences were observed between designs highlight the importance of implant selection during the planning stage of THRs, and the potential for FE models as quantitative tools that aid the implant selection process.

The findings presented should be interpreted in light of the study's limitations. The relatively small size of the cohort (16 patients) may not completely represent anatomical and physiological variations in THR patients. However, increasing variability in the cohort could only have led to larger variation in implant stability strengthening further the validity of the present conclusion. The study used a single, simplified load case representing the hip reactions and muscle forces at the time of peak hip contact force during stair ascent. While we cannot exclude that other more demanding tasks could induce higher risk of implant loosening, stair ascent loads were sufficient to induce changes in micromotion and inter-

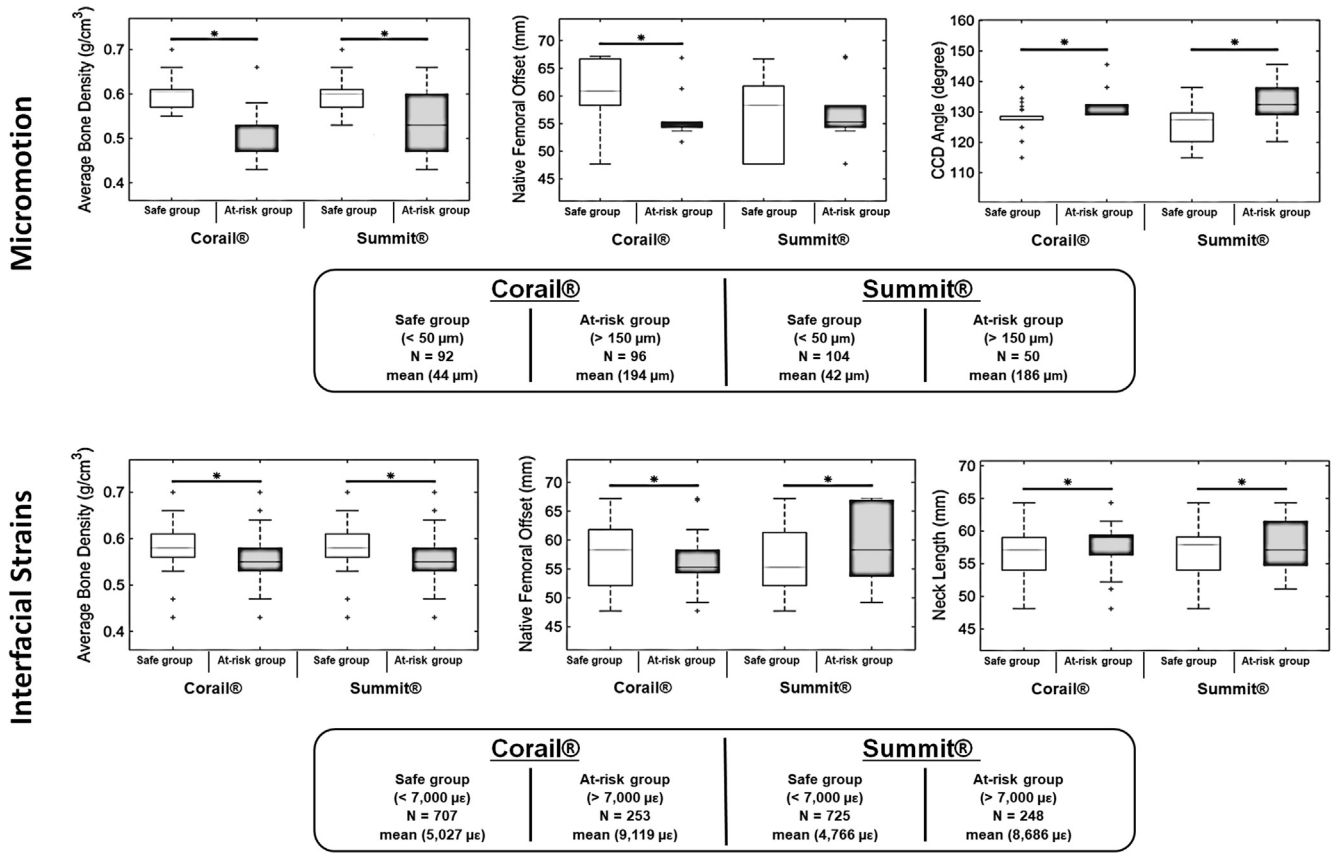

Fig. 8. Categorical comparison on patient factors based on the 90th percentile micromotion (top) and interfacial strain (bottom) categorisation. Ranges for safe and the at-risk groups are represented by the white and grey boxes, respectively. Also, the majority of implant positions resulted in implant micromotion that are greater than 50 μm and less than 150 μm, and hence were included in neither of the micromotion groups.

facial strains that are large enough to identify patient factors and implant positions that may jeopardise the primary stability of the implant (Kassi et al., 2005). The joint and muscles forces were calculated using a simplified musculoskeletal model, which scaled forces to the body mass of the patient, yet, they were not truly patient-specific. Moreover, a single boundary and loading condition was assumed to be representative of the peak joint reactions and muscle forces for the range of stem positions considered. Alteration in the head centre location are expected to induce changes in muscle and joint contact forces (Myers et al., 2018), which are expected to increase the range of variability in the peak interfacial strains, particularly for extremes bounds of the anteversion ranges explored in this study. However, for the range of implant positions considered, the magnitude of change in forces applied to the proximal femur are unlikely to introduce excessive changes to the mean and the overall micromotion/interfacial strain distributions that will significantly impact the primary stability (Amirouche et al., 2016; Heller et al., 2001). The interference due to the press-fit insertion of the implant was not modelled in this study. Interference increases the contact pressures and the shear friction at the bone-implant interface. Hence, modelling such interference is expected to reduce the micromotion and elevate the interfacial bone strains across all simulations (Abdul-Kadir et al., 2008). It was also not possible to perform direct validation for the 1952 models generated. Nonetheless, the micromotion distribution predicted by our models were in reasonable agreement (differences in median micromotion <15 μm) with previous experimental measurements taken at various regions of the femoral stem (Camine et al., 2018; Solitro et al., 2016).

In conclusion, the study confirmed the necessity to include both patient factors and surgical variation in order to fully assess the envelope of performance for femoral stems. The sensitivity of micromotion and interfacial strains varied across femora, stem positions and stem designs. However, most of the cases studied were sensitive to average BMD, CCD angle and changes in ML Offset$_{IMP}$ and Antev$_{angle}$.

Acknowledgment

This study was funded by the Australian Research Council (LP130100122) and DePuy Synthes. The authors are grateful to the staff of the Mortuary and the Donor Tissue Bank at The Victorian Institute of Forensic Medicine Australia for their assistance in collecting the material upon which this study is based. The authors are also grateful to the families of the donors who gave permission for the collection of the material expressly for research.

Conflict of interest

Prof Taylor, Prof Besier and Prof Clement are chief investigators named on the ARC linkage grant (LP130100122). Dr Al-Dirini was employed on the project. Dr Huff is employed by DePuy Synthes. All remaining authors have no conflict of interest to declare for this study.

Appendix A

(See Table A1)

Table A1
Summary of patient demographics and characteristics for the study cohort.

ID	Gender	Age	Body mass (kg)	Stature (cm)	BMI (kg/m2)	Av bone density (g/cm^{-3})	Av modulus (GPa)	Femur Length (mm)	Neck length (mm)	CCD angle (deg)	Antev (deg)	DORR	SI_femoral (mm)	ML_femoral (mm)
M1	M	68	116	178	36.6	0.7	4.0	464.1	59.2	114.9	17.7	0.7	61.8	43.2
M2	M	59	104	177	33.2	0.64	5.5	447.0	61.5	125.0	20.2	0.7	58.3	40.8
M3	M	55	94	177	30.0	0.58	5.0	495.5	64.3	131.8	7.4	0.7	67.2	46.4
M4	M	67	83	174	27.4	0.57	4.8	465.5	59.1	133.2	4.0	0.9	58.3	39.4
M5	M	56	79	176	25.5	0.58	4.9	464.3	58.3	134.4	7.9	0.9	55.2	37.6
M6	M	66	79	179	24.7	0.61	5.2	472.3	57.9	127.4	25.7	1.0	66.7	34.1
M7	M	57	72	170	24.9	0.47	4.1	449.8	57.1	132.4	25.5	0.7	55.3	30.6
M8	M	64	70	168	24.8	0.57	4.7	444.9	59.0	128.5	13.1	0.8	60.9	38.5
F1	F	59	105	169	36.8	0.58	5.1	440.3	54.0	130.8	30.3	1.0	61.3	27.8
F2	F	58	87	167	31.2	0.66	5.6	459.1	55.1	138.0	9.8	0.7	53.7	34.1
F3	F	58	81	173	27.1	0.53	4.8	454.5	59.4	129.0	16.6	0.7	54.3	38.1
F4	F	63	73	165	26.8	0.55	4.9	434.5	56.3	130.5	18.1	0.8	49.2	35.3
F5	F	57	70	151	30.7	0.56	4.9	398.9	52.2	132.6	18.3	0.7	52.1	30.8
F6	F	51	62	159	24.5	0.53	4.6	428.5	54.7	129.6	15.8	0.7	51.7	35.9
F7	F	60	62	155	25.8	0.6	4.9	412.0	48.1	120.2	5.6	0.6	47.7	35.2
F8	F	71	52	164	19.3	0.43	4.0	448.5	51.1	145.6	−3.1	0.9	66.9	26.7

References

Abdul-Kadir, M.R., Hansen, U., Klabunde, R., Lucas, D., Amis, A., 2008. Finite element modelling of primary hip stem stability: the effect of interference fit. J. Biomech. 41, 587–594.

Al-Dirini, R.M.A., O'Rourke, D., Huff, D., Martelli, S., Taylor, M., 2018. Biomechanical robustness of a successful cementless stem to surgical variation in stem size and position. Biomech Eng. 104 (9), 091007.

Al-Dirini, R.M.A., Huff, D., Zhang, J., Besier, T., Clement, J.G., Taylor, M., 2017. Influence of collars on the primary stability of cementless femoral stems: a finite element study using a diverse patient cohort. J. Orthop. Res.® 36, 1185–1195.

Amirouche, F., Solitro, G., Walia, A., 2016. No effect of femoral offset on bone implant micromotion in an experimental model. Orthop. Traumatol.: Surg. Res. 102, 379–385.

Australian Orthopaedic Association National Joint Replacement Registry, 2015. Hip and Knee Arthroplasty Annual Report Australian National Joint Arthroplasty Register, Adelaide, Australia.

Bah, M.T., Nair, P.B., Browne, M., 2009. Mesh morphing for finite element analysis of implant positioning in cementless total hip replacements. Med. Eng. Phys. 31, 1235–1243.

Bah, M.T., Nair, P.B., Browne, M., 2010. Rapid analysis of implant positioning effects in cementless total hip replacements. 17th Congress of the European Society of Biomechanics, Edinburgh, UK.

Bah, M.T., Nair, P.B., Taylor, M., Browne, M., 2011. Efficient computational method for assessing the effects of implant positioning in cementless total hip replacements. J. Biomech. 44, 1417–1422.

Bah, M.T., Shi, J., Heller, M.O., Suchier, Y., Lefebvre, F., Young, P., King, L., Dunlop, D. G., Boettcher, M., Draper, E., Browne, M., 2015. Inter-subject variability effects on the primary stability of a short cementless femoral stem. J. Biomech. 48, 1032–1042.

Bayraktar, H.H., Morgan, E.F., Niebur, G.L., Morris, G.E., Wong, E.K., Keaveny, T.M., 2004. Comparison of the elastic and yield properties of human femoral trabecular and cortical bone tissue. J. Biomech. 37, 27–35.

Bryan, R., Nair, P.B., Taylor, M., 2012. Influence of femur size and morphology on load transfer in the resurfaced femoral head: a large scale, multi-subject finite element study. J. Biomech. 45, 1952–1958.

Camine, V.M., Rüdiger, H.A., Pioletti, D.P., Terrier, A., 2018. Effect of a collar on subsidence and local micromotion of cementless femoral stems: in vitro comparative study based on micro-computerised tomography. Int. Orthop. 42, 49–57.

Clement, J.G., 2005. The Melbourne Femur Collection: the gift of tissue underpins important medical and forensic research. VIFM Rev. 3, 7–11.

Dammak, M., Shirazi-Adl, A., Schwartz Jr, M., Gustavson, L., 1997. Friction properties at the bone-metal interface: comparison of four different porous metal surfaces. J. Biomed. Mater. Res.: An Off. J. Soc. Biomater. Jpn. Soc. Biomater. 35, 329–336.

Dopico-Gonzalez, C., New, A.M., Browne, M., 2009. Probabilistic analysis of an uncemented total hip replacement. Med. Eng. Phys. 31, 470–476.

Dopico-Gonzalez, C., New, A.M., Browne, M., 2010a. A computational tool for the probabilistic finite element analysis of an uncemented total hip replacement considering variability in bone-implant version angle. Comput. Methods Biomech. Biomed. Eng. 13, 1–9.

Dopico-Gonzalez, C., New, A.M., Browne, M., 2010b. Probabilistic finite element analysis of the uncemented hip replacement–effect of femur characteristics and implant design geometry. J. Biomech. 43, 512–520.

Eskelinen, A., Remes, V., Helenius, I., Pulkkinen, P., Nevalainen, J., Paavolainen, P., 2005. Total hip arthroplasty for primary osteoarthrosis in younger patients in the Finnish arthroplasty register: 4 661 primary replacements followed for 0–22 years. Acta Orthop. 76, 28–41.

Hashemi, A., Shirazi-Adl, A., Dammak, M., 1996. Bidirectional friction study of cancellous bone-porous coated metal interface. J. Biomed. Mater. Res. 33, 257–267.

Havelin, L.I., Espehaug, B., Vollset, S.E., Engesaeter, L.B., 1995. Early aseptic loosening of uncemented femoral components in primary total hip replacement. A review based on the Norwegian Arthroplasty Register. Bone Joint J. 77, 11–17.

Heller, M.O., Bergmann, G., Deuretzbacher, G., Claes, L., Haas, N.P., Duda, G.N., 2001. Influence of femoral anteversion on proximal femoral loading: measurement and simulation in four patients. Clin. Biomech. 16, 644–649.

Heller, M.O., Bergmann, G., Kassi, J.P., Claes, L., Haas, N.P., Duda, G.N., 2005. Determination of muscle loading at the hip joint for use in pre-clinical testing. J. Biomech. 38, 1155–1163.

Kassi, J.-P., Heller, M.O., Stoeckle, U., Perka, C., Duda, G.N., 2005. Stair climbing is more critical than walking in pre-clinical assessment of primary stability in cementless THA in vitro. J. Biomech. 38, 1143–1154.

Kurtz, S., Ong, K., Lau, E., Mowat, F., Halpern, M., 2007. Projections of primary and revision hip and knee arthroplasty in the United States from 2005 to 2030. J. Bone Joint Surg. Am. 89, 780–785.

Laz, P.J., Browne, M., 2010. A review of probabilistic analysis in orthopaedic biomechanics. Proc. Instit. Mech. Eng. Part H: J. Eng. Med. 224, 927–943.

Learmonth, I.D., Young, C., Rorabeck, C., 2007. The operation of the century: total hip replacement. Lancet 370, 1508–1519.

Lengsfeld, M., Burchard, R., Gunther, D., Pressel, T., Schmitt, J., Leppek, R., Griss, P., 2005. Femoral strain changes after total hip arthroplasty - patient-specific finite element analyses 12 years after operation. Med. Eng. Phys. 27, 649–654.

Mahmood, S.S., Mukka, S.S., Crnalic, S., Wretenberg, P., Sayed-Noor, A.S., 2016. Association between changes in global femoral offset after total hip arthroplasty and function, quality of life, and abductor muscle strength: a prospective cohort study of 222 patients. Acta Orthop. 87, 36–41.

Maloney, W.J., Jasty, M., Burke, D.W., O'Connor, D.O., Zalenski, E.B., Bragdon, C., Harris, W.H., 1989. Biomechanical and histologic investigation of cemented total hip arthroplasties. A study of autopsy-retrieved femurs after in vivo cycling. Clin. Orthop. Relat. Res., 129–140

Martelli, S., Taddei, F., Schileo, E., Cristofolini, L., Rushton, N., Viceconti, M., 2012. Biomechanical robustness of a new proximal epiphyseal hip replacement to patient variability and surgical uncertainties: a FE study. Med. Eng. Phys. 34, 161–171.

Morgan, E.F., Bayraktar, H.H., Keaveny, T.M., 2003. Trabecular bone modulus-density relationships depend on anatomic site. J. Biomech. 36, 897–904.

Morgan, E.F., Keaveny, T.M., 2001. Dependence of yield strain of human trabecular bone on anatomic site. J. Biomech. 34, 569–577.

Myers, C.A., Laz, P.J., Shelburne, K.B., Judd, D.L., Huff, D.N., Winters, J.D., Stevens-Lapsley, J.E., Rullkoetter, P.J., 2018. The impact of hip implant alignment on muscle and joint loading during dynamic activities. Clin. Biomech 53, 93–100.

Pacanti, A., Bernakiewicz, M., Viceconti, M., 2003. The primary stability of a cementless stem varies between subjects as much as between activities. J. Biomech. 36, 777–785.

Pagnano, M.W., Hanssen, A.D., Lewallen, D.G., Shaughnessy, W.J., 1996. The effect of superior placement of the acetabular component on the rate of loosening after total hip arthroplasty.: long-term results in patients who have crowe type-II congenital dysplasia of the hip. JBJS 78, 1004–1014.

Pilliar, R., Lee, J., Maniatopoulos, C., 1986. Observations on the effect of movement on bone ingrowth into porous-surfaced implants. Clin. Orthop. Relat. Res. 208, 108–113.

Renner, L., Janz, V., Perka, C., Wassilew, G.I., 2016. What do we get from navigation in primary THA? EFORT Open Rev. 1, 205–210.
Russotti, G.M., Harris, W., 1991. Proximal placement of the acetabular component in total hip arthroplasty. A long-term follow-up study. J. Bone Joint Surg. Am. 73, 587–592.
Soballe, K., Toksvig-Larsen, S., Gelineck, J., Fruensgaard, S., Hansen, E.S., Ryd, L., Lucht, U., Bunger, C., 1993. Migration of hydroxyapatite coated femoral prostheses. A Roentgen Stereophotogrammetric study. J. Bone Joint Surg. [Br] 75, 681–687.
Solitro, G.F., Whitlock, K., Amirouche, F., Santis, C., 2016. Measures of micromotion in cementless femoral stems-review of current methodologies. Biomater. Biomech. Bioeng. 3, 85–104.
Taddei, F., Martelli, S., Gill, H.S., Cristofolini, L., Viceconti, M., 2010. Finite element modeling of resurfacing hip prosthesis: estimation of accuracy through experimental validation. J. Biomech. Eng. 132, 021002.
Taylor, M., Bryan, R., Galloway, F., 2013. Accounting for patient variability in finite element analysis of the intact and implanted hip and knee: a review. Int. J. Numer. Methods Biomed. Eng. 29, 273–292.
Taylor, M., Prendergast, P.J., 2015. Four decades of finite element analysis of orthopaedic devices: where are we now and what are the opportunities? J. Biomech. 48, 767–778.
Troelsen, A., Malchau, E., Sillesen, N., Malchau, H., 2013. A review of current fixation use and registry outcomes in total hip arthroplasty: the uncemented paradox. Clin. Orthop. Related Res.® 471, 2052–2059.
Umeda, N., Saito, M., Sugano, N., Ohzono, K., Nishii, T., Sakai, T., Yoshikawa, H., Ikeda, D., Murakami, A., 2003. Correlation between femoral neck version and strain on the femur after insertion of femoral prosthesis. J. Orthop. Sci. 8, 381–386.
Viceconti, M., Cristofolini, L., Baleani, M., Toni, A., 2001a. Pre-clinical validation of a new partially cemented femoral prosthesis by synergetic use of numerical and experimental methods. J. Biomech. 34, 723–731.
Viceconti, M., Monti, L., Muccini, R., Bernakiewicz, M., Toni, A., 2001b. Even a thin layer of soft tissue may compromise the primary stability of cementless hip stems. Clin. Biomech. 16, 765–775.
Viceconti, M., Muccini, R., Bernakiewicz, M., Baleani, M., Cristofolini, L., 2000. Large-sliding contact elements accurately predict levels of bone-implant micromotion relevant to osseointegration. J. Biomech. 33, 1611–1618.
Vicenti, G., Solarino, G., Spinarelli, A., Carrozzo, M., Picca, G., Maddalena, R., Rifino, F., Moretti, B., 2016. Restoring the femoral offset prevent early migration of the stem in total hip arthroplasty: an EBRA-FCA study. J. Biol. Regul. Homeost. Agents 30, 207–212.
Wechter, J., Comfort, T.K., Tatman, P., Mehle, S., Gioe, T.J., 2013. Improved survival of uncemented versus cemented femoral stems in patients aged< 70 years in a community total joint registry. Clin. Orthop. Related Res.® 471, 3588–3595.
Wong, A.S., New, A.M.R., Isaacs, G., Taylor, M., 2005. Effect of bone material properties on the initial stability of a cementless hip stem: a finite element study. Proc. Instit. Mech. Eng. Part H- J. Eng. Med. 219, 265–275.